

Stationarity and Redundancy of Multichannel EEG  
Data Recorded During Generalized Tonic-Clonic  
Seizures

Scott M. Zoldi, PhD

T-CNLS, MS B258

Los Alamos National Laboratory

Los Alamos, NM 87545; zoldi@cnls.lanl.gov

Andrew Krystal<sup>†</sup>, M.D.

Department of Psychiatry

Duke University Medical Center, Box 3309

Durham, N. C. 27708; krystal@phy.duke.edu

Henry S. Greenside<sup>†</sup>, PhD

Department of Physics, Duke University

Durham, NC 27708-0305; hsg@phy.duke.edu

May 4, 1999

## Abstract

A prerequisite for applying some signal analysis methods to electroencephalographic (EEG) data is that the data be statistically stationary. We have investigated the stationarity of 21-electrode multivariate EEG data recorded from ten patients during generalized tonic-clonic (GTC) seizures elicited by electroconvulsive therapy (ECT). Stationarity was examined by calculating probability density functions (pdfs) and power spectra over small equal-length non-overlapping time windows and then by studying visually and quantitatively the evolution of these quantities over the duration of the seizures. Our analysis shows that most of the seizures had time intervals of at least a few seconds that were statistically stationary by several criteria and simultaneously for different electrodes, and that some leads were delayed in manifesting the statistical changes associated with seizure onset evident in other leads. The stationarity across electrodes was further examined by studying redundancy of the EEG leads and how that redundancy evolved over the course of the GTC seizures. Using several different measures, we found a substantial redundancy which suggests that fewer than 21 electrodes will likely suffice for extracting dynamical and clinical insights. The redundancy analysis also demonstrates for the first time posterior-to-anterior time delays in the mid-ictal region of GTC seizures, which suggests the existence of propagating waves. The implications of these results are discussed for understanding GTC seizures and ECT treatment.

Key words: ECT, generalized seizures, stationarity, redundancy.

## I. INTRODUCTION

The analysis of multilead electroencephalographic (EEG) time series is an important but difficult goal. Such an analysis is important because the EEG provides a relatively low-cost, noninvasive way to monitor brain behavior that can yield valuable insights about brain function, pathology, and treatment. The goal is difficult because of the great complexity of brain dynamics which remains poorly understood.

For EEG data analysis, the complexity of brain dynamics manifests itself in at least three different ways. First, EEG time series are nonstationary which makes difficult the application and interpretation of many methods of signal analysis including those based on statistics [15] and nonlinear dynamics [1]. It is not understood yet how to quantify the magnitude and time-dependence of nonstationarities, how to compare the nonstationarity of one EEG recording with another, or how to identify regions of approximately stationary behavior. Second, multielectrode EEG data are spatiotemporal in character since the time series are recorded simultaneously from electrodes at different locations on the scalp. Here the relation between time series at different electrodes is not well understood, e.g., to what extent is there redundancy of the time series from different electrodes or how does one interpret the correlations that may exist. A third difficulty is the statistical variability of EEG data, which can be substantial even for EEG recorded from the same patient under presumably similar conditions. This variability complicates the extraction of features that can be used to compare one EEG with another or to classify EEG for clinical purposes.

In this paper, we apply and compare several statistical and visualization methods to quantify the stationarity and redundancy of 21-electrode EEG time series measured during generalized tonic-clonic (GTC) seizures associated with electroconvulsive therapy (ECT) treatments. Such seizures are characterized by polyspike and slow-wave activity [44] and are often observed to be nonstationary. Although nonstationarity [4, 6, 10, 16, 27] and redundancy [7, 26, 30, 31] of EEG data have been studied previously, this earlier work has not addressed GTC seizures. ECT provides a unique opportunity for the study of GTC seizures

because the seizures are induced under controlled conditions. The patient is anesthetized and given a neuromuscular relaxant (succinylcholine) which eliminates movement artifacts that would otherwise obscure the EEG data. The seizure is induced using a reproducible procedure in which a current of known amplitude and wave form is administered between two electrodes attached to particular locations on the scalp [21]. We partly address the issue of statistical variability of the EEG time series by recording and comparing ECT-induced GTC seizures from ten patients.

Our analysis of EEG data associated with GTC seizures has two goals. One is to further basic science by understanding more clearly when EEG signals may be considered stationary so that particular signal analysis methods might be applied more successfully. Our results for GTC ECT-related seizures show that several commonly used criteria for stationarity such as a power spectral density (psd) and probability distribution functions (pdfs) applied to successive windows of data often do identify the same stationary parts of the data but there are qualifications as we discuss in Section V A below. In analyzing EEG redundancy, our results further suggest that the majority of electrodes are often stationary or nonstationary together. There is a high cross-correlation between electrodes (see Eq. (4) below), which has been observed in previous EEG research but not quantified in the context of GTC seizures [7].

A second goal of this paper is to understand more specifically the electrophysiology of GTC ETC seizures. The concept of “seizure generalization” is used frequently to describe spatial aspects of ECT seizures and has been considered to be a central factor in determining the therapeutic effectiveness and side-effects associated with ECT treatments [2, 42]. For example, it has been suggested that marginal seizures are less generalized spatially [45]. Several authors have suggested that the differences in efficacy and side-effects of unilateral (UL) and bilateral (BL) ECT (the two most commonly employed electrode placements) are due to differences in generalization [2, 41, 42]. Although ECT seizures have been considered to be generalized tonic-clonic seizures [28], we observe a variation in generalization through spatial inhomogeneities of the EEG which suggest that generalization is a graded phenomenon (not

all or nothing).

Our data analysis leads to new conclusions. We quantify earlier claims [39, 43, 44] that the mean frequency of an ECT seizure decreases steadily during the seizure. (This has recently also been reported with GTC seizure EEG data using a different set of techniques based on time-varying autoregressive modeling [48].) We also identify statistical differences in ECT seizures generated by unilateral and bilateral electrode stimulation. Our statistical analysis based on time delays also provide the first evidence for wave propagation during ECT seizures. We identify evidence that seizure activity is expressed regionally in the brain and that some regions are delayed in manifesting the statistical changes characteristic of seizure activity in other leads. This variation, particularly in the temporal and pre-frontal regions, may have implications for understanding the variable cognitive side-effects and anti-depressant efficacy associated with the induced seizures.

The rest of the paper consists of the following sections. In Section II, a survey of prior work is given. In Sections III and IV, details are discussed concerning how the ECT EEG data were clinically recorded and analyzed. In Section V, we discuss our results on stationarity and redundancy. Finally, in Section VI, we summarize our conclusions and discuss some questions for further study.

## II. PREVIOUS WORK

In this Section, we review prior work with an emphasis on stationarity and redundancy. In the following Section, we discuss details of the methods that we use to measure and to analyze the ten-patient ECT EEG data set recorded at Duke University's Quantitative EEG Laboratory.

### Stationarity

Researchers have studied EEG stationarity with several methods and some of this earlier work motivated our own analysis. One method involves partitioning time series into equal-

size non-overlapping segments (typically a few seconds long), calculating power spectra for each segment, and then studying how the power spectra evolve from one segment to the next [4, 10, 16]. In another EEG study of patients in the eyes-closed waking state, researchers have compared the means of time series over successive segments and found that segments shorter than 12 seconds could often be considered stationary by this criterion [6]. Stationarity has also been studied in EEG data during sleep by testing whether there were trends over time in the signal variance [40]. Still another approach has been to compute and to compare probability distributions (pdfs) of the EEG signal over time [4, 40].

### Redundancy

Many of the studies of stationarity mentioned above concern EEG data from only one electrode and direct observation of EEG time traces indicates that not all EEG channels are stationary or nonstationary together. Although correlations and redundancy have been studied for focal epilepsies [34], researchers have not yet studied these for generalized seizures [7, 26, 31]. Instead, several authors who have studied ECT seizures have noted spatial inhomogeneities with a tendency for the EEG amplitude to be greatest in the central part of the scalp [9, 44]. An amplitude asymmetry in which electrodes on the right side have larger amplitude than those on the left has been described for right unilateral ECT (in which the stimulating electrodes are placed at the vertex and right temple) but this has not been observed for bilateral ECT (in which the electrodes are placed bi-temporally) [18, 19, 38, 39, 44, 45]. Researchers have also observed delays in the onset of seizure activity of about a second when comparing time series from two different leads [5, 39].

Some preliminary studies have analyzed the inter-hemispheric redundancy of ictal EEG data but only in two-channel data, for electrodes Fp1 and Fp2 referenced to the ipsilateral mastoid. In the 2-5 Hz frequency band, greater coherence (defined below in Eq. (4)) in the first 6 seconds after the stimulus and a lower coherence in the 6 seconds immediately after the end of the seizure have been associated with a greater likelihood of ECT therapeutic

benefit [17, 21].

Several previous studies have also employed techniques for quantifying the spatial redundancy of EEG data. Such techniques include linear correlation [30, 31], nonlinear correlation [7, 31], the average amount of mutual information [7, 25, 31], coherence [13, 23], and estimates of time-delay based on these measures [7, 13, 25, 31]. Motivated by these reports, we have studied interlead linear correlation, average amount of mutual information, and interlead time delays based on these two measures.

### III. CLINICAL METHODOLOGY

In this section, we discuss the experimental details of obtaining 21-electrode ECT EEG data. As a first step, ten subjects were studied who had been clinically referred for ECT. These subjects consisted of 6 women and 4 men with ages ranging from 45-73 years, representing a typical clinical ECT population. Prior to each treatment, the barbiturate methohexital and the muscle relaxant succinylcholine were administered at a dosage of 1 mg/kg according to standard ECT practice [3]. All subjects were free of any antidepressant, anti-convulsant, antipsychotic, or mood stabilizing medications for at least 5 days prior to the ECT course. A single seizure was recorded for each subject.

Experiments have shown that the dynamics and clinical benefits of an ECT seizure depend on the placement of the ECT electrodes on the scalp (e.g., UL or BL) and on the stimulus intensity as measured in units of the threshold intensity needed to induce a seizure [17, 20–22, 29, 36, 37]. BL ECT may be more effective, and higher-above-threshold stimuli appear to be more efficacious, particularly for UL ECT. Of the ten subjects studied in this paper, eight received pulse right unilateral ECT [8] and two received bilateral ECT. We note that the stimulus electrode placement was not controlled in this study but was determined clinically and happened to include more UL subjects. Nonetheless, this study allows a preliminary comparison of dynamical EEG differences in these two forms of treatment. Electrical stimulus dosing was administered via a standard clinical technique in

which the seizure threshold at treatment 1 was determined and then a stimulus at subsequent treatments was delivered that was a multiple (in terms of charge) of the determined threshold [47].

During the ECT treatment, twenty-one channels of EEG data (nineteen EEG leads plus two eye leads) were recorded using the International 10/20 System with locations indicated as in Fig. 2. Because of the placement of ECT stimulus electrodes, position F5 was used (midway between positions F7 and F3) as was F6 (midway between F8 and F4) but for convenience we refer to F5 and F6 throughout as leads F7 and F8. All leads were referenced to linked ears and recorded using Ag/AgCl electrodes. The data were amplified and filtered using a Nihon-Khoden 4221 device (Nihon-Khoden Corp.) with a low-frequency cutoff of 1.6 Hz and a high-frequency cutoff of 70 Hz. The data were digitized at 256 Hz with 12-bit accuracy in the form of integers between the values -2048 and 2048. Although the use of succinylcholine greatly diminishes artifacts in the EEG that would otherwise be present, some artifacts may occasionally still occur. As a result, the second author, A.D.K., carefully screened all EEG data for artifacts. Brief segments of EEG data from 2 subjects were excluded from analysis on this basis.

#### IV. METHODS FOR QUANTIFYING STATIONARITY AND REDUNDANCY

In this section, we discuss the methods that we use to analyze the ECT EEG data for stationarity and redundancy. We first discuss stationarity, for which various quantities are calculated over successive equal-sized non-overlapping time windows and over each electrode of the multivariate recording. We next discuss measures for quantifying redundancy of the multivariate EEG data and how this redundancy may evolve in time. We conclude this section by discussing how one can study whether stationarity and redundancy are affected by time-delays between a given pair of electrodes.

We note that our emphasis in using these methods is somewhat different than that of a statistician or of a nonlinear dynamicist. Since GTC seizures terminate spontaneously



1-2 minutes after induction, the corresponding EEG time series are obviously nonstationary. There are then three interesting questions. One is simply how to characterize the nonstationary dynamics so as to provide insights into the properties of a GTC seizure and this is the main emphasis of our work. A second question is whether there are significant windows of approximately stationary behavior which one could then treat by statistical and nonlinear techniques that assume stationarity. A third question, which we do not address here, is whether some hidden component of the EEG signals are statistically stationary, e.g., whether a particular filtering of the data would yield stationary behavior. Given the complexities of brain physiology and of the time series themselves (there is no known underlying mathematical model based on first principles of neuronal physiology), our analysis should be regarded as exploratory rather than intended to falsify specific hypotheses of the statistical structure of ECT EEG data.

### A. Measures of Stationarity

A statistical process is defined to be *stationary* if its statistical properties are time-translation invariant, i.e., shifting the origin of time (making the substitution  $t \rightarrow t + t_0$  where  $t_0$  is some constant) has no effect on the statistics of the process. (A weaker definition of stationarity is a process for which only the mean and variance of the process are established to be time-translation invariant.) A statistical process is *nonstationary* if any of its statistical properties depend on time [33].

Although not often stated explicitly, it should be appreciated that the definitions of stationarity and nonstationarity involve mathematical idealizations and so are impossible to establish rigorously with a finite amount of empirical data. Technically, an infinite amount of data is required to define a statistical property such as a probability distribution or joint probability distribution. Similarly, one needs infinitely many realizations to study statistical properties over some interval of time and then to examine whether those properties change with the choice of time interval.

Besides the challenge of testing the hypothesis of nonstationarity with a finite amount of data, there is a related conceptual difficulty that there is no natural measure of “degree of nonstationarity” or “magnitude of nonstationarity”. This is a simple consequence of the fact that nonstationarity is defined as the negation of stationarity, so that an arbitrarily weak time dependence of any statistical property is enough to make a time series nonstationary. One then has to look carefully at specific data and hope that certain features will suggest themselves as significant for causing nonstationary statistics.

Our approach for testing nonstationary structure was to divide all time series into successive non-overlapping equal-sized time windows (also called epochs), calculate some statistical properties of the data in each window, then study these statistical properties as a function of time (from one window to the next). Each window was chosen to be 1- or 2-seconds in length, with the length chosen qualitatively after examining visualizations of several statistical quantities as a function of time (see Fig. 3(a) as an example). These time intervals were sufficiently long to contain enough points (256 and 512 points respectively for 1- and 2-second windows) for reasonable estimates of statistical quantities yet were empirically short enough that time variations of the statistics could be examined over the typical 0.5-2 minute duration of an ECT seizure. Our results were weakly dependent on the window width over a range of 1-4 secs. In future studies, it would be useful to explore some recently proposed stationarity tests that avoid the use of windows [48].

Once a window length was determined, we used three statistical quantities to monitor possible nonstationary behavior: a window variance  $\sigma^2$ , the mean frequency  $\langle\omega\rangle$  of the power spectrum  $P(\omega)$  calculated over the time series in the window, and a  $\chi^2$  statistic that measured the deviation of the probability distribution function (pdf)  $\rho(x)$  in a given window (where  $x$  denotes the amplitude) from a cumulative pdf based on the time series of previous approximately stationary regions. In our analysis, windows were the same size and synchronized across all EEG electrodes and so each of the 19 time series of a particular EEG recording produced three new shorter time series representing the window-dependence of the above three statistical quantities. To visualize statistical trends across all 19 electrodes,

these shorter time series were next plotted as a matrix of color pixels  $M_{ij}$  by assigning a color palette to the range of the shorter time series. Each row of the matrix indicates the time dependence (from left to right) of a statistic associated with a particular electrode (see for example Fig. 3), while each column represents the values of a statistic for all electrodes in a given window.

The three statistical quantities were calculated as follows. The variance  $\sigma^2$  over a given window was calculated via the usual statistical formula

$$\sigma^2 = \frac{1}{N-1} \sum_{i=1}^N (x_i - \langle x \rangle)^2, \quad (1)$$

where  $N$  is the number of data points in a given window,  $x_i$  are the values of the EEG time series, and  $\langle x \rangle = (1/N) \sum_{i=1}^N x_i$  denotes the average value of the time series over the window.

The mean frequency  $\langle \omega \rangle$  over a given window was obtained from a frequency-weighted average of the power spectrum  $P(\omega)$  over that window:

$$\langle \omega \rangle = \frac{\sum_{j=0}^{N/2} \omega_j P(\omega_j)}{\sum_{j=0}^{N/2} P(\omega_j)}. \quad (2)$$

(The sums go from 0 to  $N/2$  because the power spectrum has only  $1 + N/2$  separate magnitudes of Fourier coefficients for a time series of length  $N$ .) The power spectrum  $P(\omega)$  over a given window was estimated with a Fast Fourier Transform [32]. Power spectra for overlapping intervals of length 2 seconds (each overlapping by 1 second) were averaged to reduce the variance of the spectrum. Each time series was also multiplied by a Parzen window before being Fourier analyzed to reduce artifacts arising from the nonperiodicity of the time series over the window [32]. The windowing of the data allowed a frequency resolution in  $P(\omega)$  of  $\Delta\omega = 0.5$  Hz. We note that the variance  $\sigma^2$  calculated for a window is proportional to the integral  $\int P(\omega) d\omega$  of the power spectrum over the window and so is not entirely independent of the power spectrum.

The pdf  $\rho(x)$  of a time series  $x_i$  in one-second-long windows was calculated by binning the data (256 points of  $x_i$ ) into 40 bins that spanned the range  $[x_{\min}, x_{\max}]$  of the minimum  $x_{\min}$  and maximum  $x_{\max}$  of the time series. Several different numbers of bins varying from 20

to 200 were studied before establishing that 40 was adequate in capturing most features of the pdf without too much statistical noise.

Since it is difficult to plot and to understand the time dependence of functions like pdfs for multivariate data and for many different electrodes, the nonstationarity of the pdfs was analyzed by plotting instead whether each pdf passed a  $\chi^2$  test [32] at the 95% level which measured the difference between the pdf in a given current window and a cumulative pdf over previous contiguous stationary windows. A cumulative pdf has the advantage of increasing the statistical accuracy when comparing a new pdf with a previous standard. (Recently Witt et al [49] also suggested using a  $\chi^2$  test for pdfs to quantify nonstationarity in a time series, but they did not use a cumulative pdf as we do here.)

The  $\chi^2$  value for a particular window was calculated as follows. If  $M$  denotes the number of bins (here  $M = 40$ ), and  $n_i$  and  $N_i$  denote respectively the number of points in the  $i$ th bin of the current and cumulative pdfs, then we calculated the number [32]

$$\chi^2 = \sum_{i=1}^M \frac{(n_i - N_i)^2}{(n_i + N_i)}. \quad (3)$$

Nonstationarity was then visualized by assigning values of 0 and 1 to windows that respectively failed and passed the  $\chi^2$  test. A visualization of such  $\chi^2$  values as a function of window index  $i$  is given in Fig. 4 and discussed further below in Section V A.

## B. Redundancy and Time Delays

Redundancy of the 19 electrode time series and of statistics calculated for the 19 electrode time series were quantified using linear correlation coefficients and mutual information, with large values of these quantities corresponding to substantial redundancy. The linear correlation coefficients  $r_{xy}$  between two time series  $x_i$  and  $y_i$  were estimated from the sample correlation coefficient defined as follows [15, 32]:

$$r_{xy} = \frac{\sum_{i=1}^N (x_i - \langle x \rangle) (y_i - \langle y \rangle)}{\sqrt{\sum_{i=1}^N (x_i - \langle x \rangle)^2} \sqrt{\sum_{i=1}^N (y_i - \langle y \rangle)^2}}. \quad (4)$$

In this paper we studied the 18 correlation coefficients  $r_{x,CZ}$  of all electrodes with the centrally located electrode CZ. The choice of CZ was motivated by earlier work [44] which showed that ECT EEG signals are often largest in amplitude in an apparently highly correlated region centered around lead CZ. The use of this lead in analyses of redundancy of other leads thus helped to test when leads were highly related to the dominant activity. The 18 coefficients  $r_{xy}$  giving the time-evolution of redundancy with electrode CZ were computed over a segment of the EEG where at least 15 electrodes were simultaneously stationary.

Since it is known from studies in nonlinear dynamics that linear coefficients such as Eq. (4) sometimes miss nonlinear correlations [24], we supplemented our analysis of cross-correlation by studying the mutual information of pairs of time series [11, 24, 26]. If the quantities  $\rho_x(x)$  and  $\rho_y(y)$  denote the pdfs for two time series  $x_i$  and  $y_i$  on a given window and if  $\rho_{xy}(x, y)$  denotes the joint pdf (estimated numerically by sorting pairs of points  $(x_i, y_i)$  simultaneously into 40 bins spanning the  $x$ -range and 40 bins spanning the  $y$  range), then the mutual information  $I(x, y)$  is defined to be [11]:

$$I(x, y) = \sum_{i=1}^N \sum_{j=1}^N \rho_{xy}(x_i, y_j) \log \left( \frac{\rho_{xy}(x_i, y_j)}{\rho_x(x_i)\rho_y(y_j)} \right). \quad (5)$$

For statistically independent time series, the joint distribution  $\rho_{xy}(x, y) = \rho_x(x)\rho_y(y)$  factors into a product of the separate pdfs and  $I(x, y)$  becomes zero. Empirically we found that 2-second windows contained enough data to generate good approximate joint probability distributions; if larger segments of data were studied the time evolution of redundancy could not be studied. Mutual information coefficients between electrode CZ and the other 18 leads were calculated every 2 seconds to obtain their time dependence over the seizure.

All interlead time-averaged linear correlation and mutual information coefficients were calculated over “global” stationary regions determined by the stationarity tests indicated above. These global stationary regions were identified visually as the largest continuous part of the time series that was stationary for the majority of electrodes. The average interlead coefficients between all pairs of electrodes were represented in a  $19 \times 19$  square matrix. These matrices allowed us to determine the average redundancy between one lead and all

other leads in the seizure using both linear correlations and mutual information (see Figs. 8 and 9).

The correlation function Eq. (4) and the mutual information Eq. (5) were also used to measure time-delays between two time series  $x_i$  and  $y_j$  associated with two different electrodes. To compute the time-delay, one time series  $y_i$  was fixed and the second series  $x_i$  waveform was then shifted in time from -40 ms to 40 ms (corresponding to integer shifts  $x_{i+k}$  of  $k = -10$  and  $k = +10$ ) to find the time-delay that resulted in the maximum value of the mutual information. We then determined the shift that gave the largest redundancy according to Eq. (4) or Eq. (5). To reduce the large number of inter-lead comparisons, time-delays were again calculated only for leads paired with the central electrode CZ. We found 2-second or larger stationary segments of uniform time-delay in one half of the seizures. In Fig. 10, we display the time-average of the time-delays over a global stationary region over the surface of the head.

## V. RESULTS AND DISCUSSION

### A. Stationarity

#### 1. Signal Variance Over Time

By using plots similar to Fig. 3 to examine all 10 seizures, we found a substantial variation between seizures in the pattern and degree of stationarity, as measured by the signal variance. Figs. 3a and 3b are representative of the diversity of variance evolution that was present across these seizures. Fig. 3a illustrates that the variance remains relatively low for the first 18 seconds of the seizure in all leads and then increases (as indicated by the change from blue and green to yellow and red) for the fourteen seconds thereafter, but only in the fronto-central region of the head (leads FP1, F3, FZ, CZ, FP2, and F4). This behavior is typical of the increase in amplitude that has previously been described in the transition from the early tonic phase of the seizure to the later larger amplitude mid-ictal poly-spike

and wave EEG pattern characteristic of the clonic phase of generalized tonic-clonic seizures, which is largest in amplitude in the fronto-central region [21, 44, 46]. Fig. 3(a) also manifests two periods of apparent stationarity of signal amplitude in that for times 2-16 (a 14-second segment) and times 20-32 (a later 12-second segment) there is minimal change in the color of the figure in any channel.

In contrast, Fig. 3b is a seizure whose variance is three times smaller and that has briefer segments of amplitude stationarity. There are a number of approximately 5-second segments that appear to maintain consistent variance across the head but not longer stationary segments. The amplitude is once again greatest fronto-centrally but only intermittently.

To better illustrate the range of variance stationarity present, we note that for 8 of 10 seizures, stationary segments of 8 seconds or longer could be identified where there was little change in the signal variance in any lead. The other two seizures had highly variable variance as shown in Fig. 3b. The largest stationary segment present in a single-lead in any of the seizures was 80 seconds. The largest segment that was stationary across all of the leads was 30 seconds in length.

There was some consistency across the seizures in the spatial and temporal patterns of variance. The fronto-central leads tended to be larger in amplitude than the temporal and occipital leads in nine of ten of the seizures including both unilateral and bilateral seizures. For most leads the variance increased from the start of the seizure to the mid-ictal portion, however this increase was relatively delayed in the onset of the temporal and occipital leads. For 6 of the 10 seizures, the time at which the variance increased was delayed in at least one lead for both unilateral and bilaterally induced seizures. In some of the seizures a few leads never manifested an increase in variance. This can be seen in Fig. 3a where T4, T6, T3, T5, P3, O1, O2, and F8 do not appear to increase in amplitude and in Fig. 3b where there does not appear to be an increase for leads T3 and T5.

We conclude that the variance indicates a range of amplitude stationarity for generalized tonic-clonic seizures. For most seizures (eight of ten) a region of stationarity of at least 8 seconds can be expected for all leads, however there are some seizures where only much

brief periods of amplitude stationarity can be found. These analyses also indicate that the signal amplitude tends to be greatest, and that there is an earlier onset in increased variance, in the fronto-central as compared with temporal and occipital leads and occasionally frontopolar leads.

## 2. $\chi^2$ Stationarity Test

Fig. 4(a) and Fig. 4(b) depict the results of the  $\chi^2$  stationarity test for two seizures, which are again representative of the range of observed stationarity phenomena. These figures utilize the same format as the variance evolution figures except that black and white pixels are now used to indicate whether the pdf of a new EEG epoch was or was not distinct from the accumulated pdf for previous epochs at the 95% confidence level.

The  $\chi^2$  test results for the seizure depicted in Fig. 3(b) appear in Fig. 4(a). While the data in Fig. 3(b) are relatively nonstationary by the variance analysis, they are not obviously nonstationary using the  $\chi^2$  measure, so that there are differences between these measures of stationarity. In Fig. 3(a), leads O2, T3, T5, T4, T6 and O1 have the longest stationary single-lead segments during a seizure lasting about 16-40 seconds, which is consistent with these leads not demonstrating an increase in variance over the seizure. Regions of global stationarity as identified by the  $\chi^2$  test were found in all seizures, with the shortest global segments observed in two unilateral seizures (e.g., see Fig. 4(b) where no stationary segments were observed longer than a few seconds for all leads). The range in length of the stationary segments over all leads was 4 to 30 seconds. All of the seizures had single-lead stationarity segments of at least 10 seconds, with the longest single-lead stationary segment lasting 70 seconds. Fifteen second or larger segments of multi-lead stationarity were found in half of the seizures.



### *3. Average Power Spectral Frequency*

We found that the pdf nonstationarity tests and regions of uniform frequency generally agreed with one another. Fig. 5a displays the average frequency over time for the same seizure depicted in Fig. 3a and indicates a 10-second region of nearly constant multi-lead frequency from 10-20 seconds. In contrast, Fig. 5b has single leads with long times of stationary average frequency but this is not seen across all of the leads. Leads FP1 and O2 have greater variation in frequency across the seizure and have, in general, higher average frequency content. The average frequency for both of these seizures decreases over the seizure. However, in Fig. 5b, this decrease does not seem to occur for leads FP1 and O2. In fact, for seven of the ten seizures, at least one lead was delayed in decreasing frequency or did not manifest a decrease in frequency over the seizure. This was most commonly seen in the temporal, occipital, and frontopolar leads. Across all of the seizures, fifteen second or longer regions of uniform frequency in all leads were found in six of the ten seizures. Five of ten seizures had many brief global average frequency nonstationarities and these corresponded to nonstationarities detected by the pdf nonstationarity tests, e.g., time 21 seconds in Fig. 5a.

#### *Summary Of Stationarity Analysis*

A substantial variability was found in the length of stationary segments across the seizures studied. For most of the seizures, there were substantial windows of approximately stationary behavior observed in all leads simultaneously, using several different criteria. Significant differences between the measures were found suggesting that stationarity according to one of the criteria does not insure stationarity by another criteria. Some of the seizures studied did not have multi-lead stationarity segments longer than a few seconds, which suggests that there are likely to be problems when applying signal analysis techniques that assume signal stationarity for generalized tonic-clonic seizure data. On the other-hand,

since these analyses indicate that stationary segments exist for the vast majority of these seizures, such analytic techniques may be validly applied after first verifying that they are being applied to a segment that is stationary according a range of stationarity tests. For both unilateral and bilateral seizures, these analyses also indicate that there may be leads that are delayed in demonstrating statistical changes such as an increase in signal variance or a decrease in average frequency as compared with other leads. This was seen most commonly in temporal, occipital, and prefrontal regions.

## B. Redundancy

### 1. Time Evolution Of Mutual Information Transmission Coefficient

The time evolution of mutual information for each lead were calculated with respect to the lead CZ. (As discussed above, CZ was picked because of prior reports suggesting that ECT-induced seizures tend to be maximal in amplitude in this region [44]. However we verified that the results were the same when mutual information was studied with respect to a number of different leads.) The time evolution of mutual information over the course of two seizures that illustrate the range of phenomena seen in the 10 seizures are depicted in Fig. 6a and Fig. 6b. As in previous figures, the amount of mutual information shared between each lead and CZ is represented by color pixels whose magnitude is indicated in the color bar below each figure.

The ten seizures varied substantially in the spatiotemporal pattern of redundancy as measured with mutual information. Fig. 6a illustrates a seizure with high redundancy of CZ with most other leads, whereas Fig. 6b depicts a seizure with little inter-lead redundancy with CZ, even though this seizure has a large stationary region. Fig. 6a also demonstrates that over the course of the seizure there is a transition from a period of relatively low-interlead redundancy to increased redundancy where the greatest inter-lead redundancy, like the greatest variance, is in the fronto-central region. The increase in redundancy and

amplitude, although not manifest in all seizures, coincides with the transition from the tonic to clonic phases of the seizures [44]. In addition, as with variance and average frequency, some leads are late to increase in redundancy or do not do so at all. This was true for 5 of the 10 seizures and most often occurred in the temporal and occipital leads.

The mutual information also provided information about the redundancy of stationarity for the EEG data. There was a period of uniform redundancy for 6 of the 10 seizures ranging from 10 to 20 seconds in length. These regions were located in the mid-ictal region of the seizure, coinciding with the clonic phase. The regions of constant redundancy across the leads coincided with regions where CZ was stationary and also where the frequency content of all the leads was nearly uniform.

## *2. Correlation Coefficient*

The amount of redundancy among seizures was also studied by calculating the time-evolution of the correlation coefficient of each lead with CZ. Two seizures illustrating the range of patterns of inter-lead correlation among the ten seizures appear in Fig. 7a and Fig. 7b. Similar phenomena are seen with the correlation coefficient as with mutual information. All leads have low redundancy initially followed by an increase in the mid-ictal period, with the greatest redundancy among the fronto-central leads with correlation coefficients ranging from 0.7-0.95. Some leads are late to increase or never increase in redundancy. In both of the figures, this occurs most prominently for the fronto-polar, temporal, and occipital leads. Late onset of an increase in redundancy occurred in 8 of the 10 seizures and was most consistent and most pronounced in the occipital and temporal leads. In terms of the stationarity of redundancy, there were regions of uniform correlation for 5 of 10 seizures ranging from 10 to 20 seconds in length. As discussed below, one factor that must be considered for accounting for leads with decreased redundancy is the possibility of a phase lag between the signals in the leads studied.

### *3. Average Mutual Information For Stationary Midictal Segments*

Average mutual information calculations were performed on regions that were found to be stationary as determined by the  $\chi^2$  nonstationarity test. Stationary regions were identified that were 6 to 20 seconds in length within the mid-ictal portions of each seizure. The average mutual information for two seizures, that are representative of the phenomena we observed among the ten seizures, is depicted in Fig. 8a and Fig. 8b. In these figures, the darkness of the square at the intersection of two lead labels indicates the mutual information shared by those leads. The correspondence between the degree of shading and the degree of redundancy is indicated by the scale at the left of the figure. Note that the same information is portrayed in the upper left and lower right halves of these figures.

Once again we found that the greatest interlead redundancy tended to occur in the frontocentral regions. The regions of highest redundancy tended to differ for UL- (see Fig. 8a) and BL-induced ECT seizures (see Fig. 8b). There tended to be increased redundancy in the right (stimulated) hemisphere for UL ECT (note the clustering of lighter boxes in the lower left and upper right corners of Fig. 8a), whereas for BL ECT the redundancy was not localized to either hemisphere. The regions of lowest redundancy were the occipital and left temporal leads in all unilateral seizures. In bilateral seizures, all temporal and occipital leads had lowered redundancy with no hemisphere dependence.

### *4. Inter-Lead Correlation For Stationary Midictal Segments*

The same global stationary regions utilized for average mutual information analysis were also used for the average correlation coefficient calculations. Two representative seizures are depicted in Fig. 9a and Fig. 9b. Relatively weaker correlations of the frontal-polar and occipital leads (see the bands of darkly shaded squares associated with these leads in Fig. 9a and Fig. 9b) with other leads on the scalp were found in seven of ten seizures with the frontal polar regions having the poorest correlations. In some cases, these leads have poor

correlations due to the presence of large time-delays with other leads on the head (see below). Lowered redundancy for the frontopolar leads in Fig. 9b was not indicated by the mutual information measure for the same seizure Fig. 8b since mutual information was less sensitive to time delays. A reduced redundancy was thus found particularly for the frontopolar and occipital leads in the midictal period. In some instances, this was due to time delays but, in several other cases, the data in the leads were not as well related.

### C. Interlead Time Delays

A number of leads had sustained poor redundancy with CZ because of time delays with CZ, which artificially lowered the apparent redundancy in our correlation analysis. This is seen in 6 of 10 seizures in leads FP1, FP2, O1, and O2 (see Fig. 7a). In contrast, Fig. 7b illustrates an instance where leads O1, O2, FP1, and FP2 have poor correlations with CZ for reasons other than time delays. Because of the dynamical and physiological importance of consistent time delays across the head in the midictal period, we sought to understand this phenomenon more thoroughly as we now discuss.

The time delay calculation cannot be calculated for data where the leads have a low redundancy since if two leads are not related, then their time delay has no meaning. As a result, we required that segments meet the  $\chi^2$ -stationarity criterion, be of constant average frequency by visual inspection, and have interlead redundancy of at least 0.5 as measured by mutual information. We first studied time delay over the course of the seizures. Segments of uniform nonzero time-delay over many leads were identified in 7 of the 10 seizures studied and they lasted between 4 and 20 seconds. The most consistent pattern in time delays was a large delay from the front to the back of the head. This pattern was found in 4 of the 10 seizures, and the magnitude of the delay ranged from -10 to 15 ms. The occipital leads had a negative time delay with CZ whereas the prefrontal leads had a positive time delay.

The average amplitude of the time delay with respect to CZ across the head for one representative mid-ictal segment is mapped in Fig. 10. This map depicts the time delay

with respect to CZ for the 19 scalp leads such that the color at each point indicates the degree of time delay based on the scale at the bottom of the figure. Data is mapped at the 19 white marks corresponding to lead location with linear interpolation in between leads. This figure illustrates what appears to be a consistent frontal-to-occipital time delay indicative of wave-like propagation from the occipital to prefrontal regions during the mid-ictal portion of some seizures. In some instances we observed a tendency for counter-clockwise rotations around CZ. While this wave phenomena was mapped for a brief period, it could be observed for over 20 seconds.

## VI. CONCLUSIONS

In this paper, we have studied the stationarity and redundancy of multielectrode EEG data during GTC seizures. Stationarity of EEG data is a main concern in gaining insights to the underlying dynamics. Reliable statistical analysis and many nonlinear measures of complexity assume statistically stationary data. We find that the use of variance non-stationarity tests, pdf non-stationarity tests, and average-frequency evolution may provide a useful measure of the stationarity in these signals. Global regions of stationary data are of length 8 to 20 seconds in the majority of seizures and single lead stationary regions are typically of length 20 to 40 seconds. Highly non-stationary seizures tend to have higher variance and show no global regions of stationarity. In prior work, we have found that seizures which had a more predictable EEG pattern over time (according to the largest Lyapunov exponent) were more therapeutically effective [22]. Further work would be useful to establish whether the more stationary seizures are also more beneficial in the treatment of depression.

Redundancy on the surface of the head varies among patients and is further complicated by nonstationarities and leads that are late or never enter into the seizure activity. We find that the mutual information statistic is much more robust to time-delays between different leads than linear correlation measures. The frontal region of most seizures along

the excitatory current path tends to have sustained higher redundancies than other portions of the head. More interesting is the high redundancy seen in some seizures among spatially distant portions of the head. In the majority of seizures, the frontal and occipital regions are poorly redundant. However, in three seizures we find high redundancy between different pairings of anterior and posterior leads. High redundancy pairings, O2-FP1 and O2-F8, seen in some seizures are not understood. In all seizures, the redundancy tends to increase in the later mid-ictal portions of these seizures. This also coincides with seizures exhibiting more rhythmicity and spatial wave behavior.

The wave-like behavior in the EEG which we have observed in GTC seizures has not been previously reported. This behavior could be caused collectively by the coupling of dynamically different parts of the brain, leading to a wave that propagates cyclically through the brain tissue. Alternatively, one region of the brain may be a source that drives the observed seizure activity in other parts of the brain. Unfortunately, physiologic evidence is presently lacking that can determine the mechanism of this wave-like electrical activity pattern. Identification and characterization of such cortical waves may be possible by using a complex Karhunen-Loève decomposition [14], which has been used successfully by meteorologists to identify wave motion in the atmosphere. Such analysis may help to determine how frequently wave motion occurs in GTC seizures and to explain the mechanism of electrical propagation of activity in these seizures.

The occurrence of surface waves on the cortex of the head and the fact that many seizures have leads that are late or that never enter into the seizure evolution call into question the utility of the term “generalized” in describing GTC seizures. There is evidence that sometimes the seizure spreads from the frontal region to the occipital and temporal regions of the head. Also, some leads can be as late as 10 seconds to enter into the seizure or do not participate in the seizure. Late-to-generalize seizures have been previously reported [5], but leads not involved in the seizure have not previously been described and the clinical relevance of these uninvolved leads remains to be established.

These findings speak against the view that GTC seizures are an instantaneous all-out

response of the brain. Instead they are consistent with prior work indicating that GTC seizures are graded rather than maximal responses [28]. Such work involved the demonstration that the cerebellum and the lower brainstem had varying degrees of electrophysiological involvement in GTC seizures in the cat and that the visual evoked response was variably disrupted in GTC seizures in humans [35]. The findings of the present study demonstrate that such variability is manifest in the EEG signals recorded during GTC seizures as well. In addition, there is evidence that there are complex spatiotemporal dynamics involved in the development and propagation of these seizures. Such results speak against the sudden onset of massive discharge in reticular structures that was once proposed [12] and more for a graded, diffusive model for the origin and spread of GTC seizure activity.

In summary, our analysis of the stationarity and redundancy of multichannel EEG data recorded during GTC seizures has identified numerous new features and these have implications for further research. First, there is a substantial variability in stationarity. Techniques that assume stationarity should be applied only after verifying that a given time segment is acceptably stationary. The variability in stationarity suggests a need for further studies that could determine the relationship of the degree of nonstationarity of GTC seizures to their antidepressant efficacy. We also found a variation in redundancy between the leads, with the greatest redundancy in fronto-central regions with decreased pre-frontal, temporal and occipital redundancy. Further work to determine the physiology underlying this differential spatial redundancy will be important for understanding GTC seizures as will attempts to determine whether diminished redundancy in particular regions is associated with diminished therapeutic efficacy or side-effects of ECT. These same regions are also apparently delayed at times in entering the seizures suggesting a more complex spatio-temporal evolution than previously reported, which is another feature that will be important for understanding the physiology and antidepressant efficacy of these seizures. Complex spatiotemporal dynamics is also suggested by evidence of wave-like behavior. All of these observations point to graded, rather than all or none physiologic phenomena underlying GTC seizures and will be important bases for new models of GTC seizures and in better understanding and improving



ECT treatment.

### ACKNOWLEDGEMENTS

This work was supported by grants NSF-CDA-91-23483 and NSF-DMS-93-07893 of the National Science Foundation, by grant DOE-DE-FG05-94ER25214 of the Department of Energy, by grants K20MH01151 and R29MH57532 of the National Institute of Mental Health, and by a Computational Science Graduate Fellowship Program of the Department of Energy.

## REFERENCES

- † Also Center for Nonlinear and Complex Systems, Duke University, Durham, N. C.
- [1] H. D. Abarbanel, R. Brown, and L. S. Tsimring. The analysis of observed chaotic data in physical systems. *Rev. Mod. Phys.*, 65(4):1331–1392, 1993.
  - [2] R. Abrams. Seizure generalization and the efficacy of unilateral ECT. *Convulsive Therapy*, 7:213–217, 1991.
  - [3] American Psychiatric Association, Washington, DC. *The Practice of ECT: Recommendations for Treatment, Training, and Privileging*, 1990.
  - [4] J. S. Barlow. Methods of analysis of nonstationary EEGs, with emphasis on segmentation techniques: A comparative review. *J. Clin. Neurophysiology*, 2:267–304, 1985.
  - [5] R. A. Brumback and R. D. Station. The electroencephalographic pattern during electroconvulsive therapy. *Clin. Electroenceph.*, 13:148–153, 1982.
  - [6] A. B. Cohen and A. Sances. Stationarity of the human electroencephalogram. *Med. & Biol. Eng. & Comput.*, 15:513–518, 1977.
  - [7] F. Lopes da Silva, J. P. Pijn, and P. Boeijinga. Interdependence of EEG signals: linear vs. nonlinear associations and the significance of time delays and phase shifts. *Brain Topography*, 2(1/2):9–18, 1989.
  - [8] G. d’Elia. Unilateral electroconvulsive therapy. *Acta Psychiatr. Scand. Suppl.*, 46:30–97, 1970.
  - [9] J. D. Enderle, R. D. Staton, J. W. Gerst, C. E. Barr, and R. A. Brumback. The electroencephalographic pattern during electroconvulsive therapy III. Analysis of frontotemporal and nasopharyngeal spectral energy. *Clinical Electroencephalography*, 17:66–77, 1986.
  - [10] G. Ferber. Treatment of some nonstationarities in the EEG. *Neuropsychobiology*, 17:100–104, 1987.

- [11] Andrew M. Fraser. Information and entropy in strange attractors. *IEEE Trans. Info. Theory*, 35(2):245–262, 1989.
- [12] H. Gastaut and R. Broughton. *Epileptic Seizures*. Charles C. Thomas, Springfield, IL., 1972.
- [13] J. Gotman. Interhemispheric relations during bilateral spike-wave activity. *Epilepsia*, 22:453–466, 1981.
- [14] J. D. Horel. Complex Principal Component Analysis: Theory and Examples. *J. Climate and Applied Meteorology*, 23:1660–1673, 1984.
- [15] Richard A. Johnson and Dean W. Wichern. *Applied Multivariate Statistical Analysis*. Prentice Hall, Englewood Cliffs, NJ, third edition, 1992.
- [16] N. Kawabata. A nonstationary analysis of the electroencephalogram. *IEEE Trans. Biomed. Eng.*, 20:444–452, 1973.
- [17] A. D. Krystal, R. D. Weiner, and C. E. Coffey. The ictal EEG as a marker of adequate stimulus intensity with unilateral ECT. *J. Neuropsychiatry and Clin. Neurophysiol.*, 7:295–303, 1995.
- [18] A. D. Krystal, R. D. Weiner, C. E. Coffey, P. Smith, R. Arias, and E. Moffett. EEG evidence of more ‘intense’ seizure activity with bilateral ECT. *Biological Psychiatry*, 31:617–621, 1992.
- [19] A. D. Krystal, R. D. Weiner, W. V. McCall, F. E. Shelp, R. Arias, and P. Smith. The effects of ECT stimulus dose and electrode placement on the ictal electroencephalogram: An intra-individual cross-over study. Submitted, 1993.
- [20] A. D. Krystal, S. Zoldi, H. Greenside, R. Prado, M. West, and R. Weiner. The effects of ECT on the EEG: implications for rTMS. To be published, 1999.
- [21] Andrew Krystal, Henry Greenside, Richard D. Weiner, and Daniel Gassert. A compar-

- ison of EEG signal dynamics in waking, after anesthesia induction and during ECT seizures. *Electroencephalography and Clinical Neurophysiology*, 99:129–140, 1996.
- [22] Andrew D. Krystal, Craig Zaidman, Henry S. Greenside, Richard D. Weiner, and C. Edward Coffey. The largest Lyapunov exponent of the EEG during ECT seizures as a measure of ECT seizure adequacy. *Electroencephalography and Clinical Neurophysiology*, 103:599–606, 1997.
- [23] A. F. Leuchter, T. F. Newton, I. A. Cook, and D. O. Walter. Changes in brain functional connectivity in alzheimer-type and multi-infarct dementia. *Brain*, 115:1543–1561, 1992.
- [24] Wentian Li. Mutual information functions versus correlation functions. *J. Stat. Phys.*, 60(5/6):823–837, 1990.
- [25] N. J. I. Mars, P. M. Thompson, and R. J. Wilkus. Spread of epileptic seizure activity in humans. *Epilepsia*, 26:85–94, 1985.
- [26] N. J. I. Mars and G. W. van Arragon. Time delay estimation in nonlinear systems using average amount of mutual information analysis. *Signal Processing*, 4:139–153, 1982.
- [27] Gottfried Mayer-Kress. Localized measures for nonstationary time-series of physiological data. *Integrative Physiological and Behavioral Science*, 29(3):205–210, 1994.
- [28] E. Niedermeyer. Epileptic seizure disorders. In E. Niedermeyer and F. Lopes da Silva, editors, *Electroencephalography: Basic Principles, Clinical Applications, and Related Fields*, pages 461–564, Baltimore, MD, 1993. Williams and Wilkins.
- [29] M. S. Nobler, H. A. Sackeim, M. Solomou, B. Lubner, D. P. Devanand, and J. Prudic. EEG manifestations during ECT: Effects of electrode placement and stimulus intensity. *Biol. Psychiatry*, 34:321–330, 1993.
- [30] G. Pfurtscheller. Some results of the analysis of epileptic seizure patterns by correlation-methods. In Petsche and Brazier, editors, *Synchronization of EEG Activity in Epilepsies*,

pages 286–290, New York, 1971. Springer Verlag.

- [31] J. P. M Pijn, P. C. M. Vijn, F. H. Lopes da Silva, W. Van Ende Boas, and W. Blanes. Localization of epileptogenic foci using a new signal analytic approach. *Neurophysiol. Clin.*, 20:1–11, 1990.
- [32] W. H. Press, S. A. Teukolsky, W. T. Vetterling, and B. P. Flannery. *Numerical Recipes in C, Second Edition*. Cambridge University Press, New York, 1992.
- [33] M. B. Priestley. *Nonlinear and Nonstationary Time Series Analysis*. Academic Press, London, 1988.
- [34] Michel Le Van Quyen, Jacques Martinerie, Claude Adam, and Francisco J. Varela. Nonlinear analyses of interictal EEG map the brain interdependences in human focal epilepsy. *Physica D*, 127:250–266, 1999.
- [35] E. A. Rodin, S. Gonzales, D. Caldwell, and D. Laginess. Photic evoked responses during induced epileptic seizures. *Epilepsia*, 7:202–214, 1966.
- [36] H. A. Sackeim, D. P. Devanand, and J. Prudic. Stimulus intensity, seizure threshold, and seizure duration: Impact on the efficacy and safety of ECT. *Psychiatric Clin. North Am*, 14:803–843, 1991.
- [37] H. A. Sackeim, J. Prudic, D. P. Devanand, J. E. Kiersky, L. Fitzsimons, B. J. Moody, M. C. McElhiney, E. A. Coleman, and J. M. Settembrino. Effects of stimulus intensity and electrode placement on the efficacy and cognitive side-effects of electroconvulsive therapy. *New Eng. J. Med.*, 328:839–846, 1993.
- [38] J. G. Small, I. F. Small, H. C. Perez, and P. Sharpley. Electroencephalographic and neurophysiological studies of electrically induced seizures. *J. Nerv. Ment. Dis*, 150:479–489, 1970.
- [39] R. D. Staton, P. J. Hass, and R. A. Brumback. Electroencephalographic recording during

- bitemporal and unilateral non-dominant hemisphere (Lancaster position) electroconvulsive therapy. *J. Clin. Psychiatry*, 42:264–269, 1981.
- [40] Hideyuki Sugimoto, Naohiro Ishii, Akira Iwata, and Nobuo Suzumura. On the stationarity and normality of the electroencephalographic data during sleep stages. *Computer Programs in Biomedicine*, 8:224–234, 1978.
- [41] C. M. Swartz. Generalization, duration, and low-frequency electroencephalographic persistence of bilateral electroconvulsive therapy seizure. *Biological Psychiatry*, 38(12):837–842, 1995.
- [42] C. M. Swartz and G. Larson. Generalization of the effects of unilateral and bilateral ECT. *Am. J. Psychiatry*, 143:1040–1041, 1986.
- [43] R. D. Weiner. EEG related to electroconvulsive therapy. In J. R. Hughes and W. P. Wilson, editors, *EEG and Evoked Potentials in Psychiatry and Behavioral Neurology*, pages 101–126. Butterworth, Boston, MA, 1983.
- [44] R. D. Weiner, C. E. Coffey, and A. D. Krystal. The monitoring and management of electrically induced seizures. In C. Kellner, editor, *Psychiatric Clinics of North America*, volume 14, pages 845–869, New York, 1991. W. B. Saunders.
- [45] R. D. Weiner and A. D. Krystal. EEG monitoring of ECT seizures. In C. Edward Coffey, editor, *The Clinical Science of Electroconvulsive Therapy*, pages 93–109, Washington, DC, 1993. American Psychiatric Press.
- [46] R. D. Weiner and A. D. Krystal. Eeg monitoring of ECT seizures. In *The clinical Science of Electroconvulsive Therapy*, pages 93–109, Washington, DC, 1993. American Psychiatric Press.
- [47] R. D. Weiner and A. D. Krystal. The present use of electroconvulsive therapy. *Annual Review of Medicine*, 45:273–281, 1994.

- [48] M. West, R. Prado, and A. D. Krystal. Evaluation and comparison of EEG traces: Latent structure in nontationary time-series. *J. American Stat. Assn.*, in press, 1999.
- [49] A. Witt, J. Kirths, and A. Pikovsky. Testing stationarity in time series. *Phys. Rev. E*, 58(2):1800–1810, 1998.

## FIGURES

FIG. 1. Ten seconds of 19 channel ictal EEG data recorded during the middle portion of two ECT seizures. The vertical lines indicate one second intervals, the vertical axis is voltage in microvolts. **(a)** A representative seizure that has a more stationary mid-seizure EEG pattern and higher redundancy among the leads. **(b)** A representative seizure that has a relatively lower stationarity and interlead redundancy.

FIG. 2. The location on the head of the 19 EEG leads according to the International 10-20 System. These are displayed in a two-dimensional representation looking down on top of the head.

FIG. 3. Variance  $\sigma^2(t)$  versus time  $t$  for seizures A and B. The period of postictal suppression following the end of the seizures is excluded from all figures and occurred just following the period depicted in the figures. (Epochs are in units of 2 secs). **(a)** Variance evolution for BL ECT seizure A with a 15-second stationary segment from  $t = 0$  to  $t = 15$ . The highest variance is seen in FZ and PZ. Leads T6, T4, O2, O1, and T5 have lower variances and are late to enter the seizure. **(b)** The variance evolution for BL seizure B shows both an initial stationary region and global regions of nonstationarity at epochs 13, 19, and 21.

FIG. 4. **(a)** Nonstationarity pdf test for BL seizure B, based on a comparison of probability distribution functions (pdfs) using a  $\chi^2$ -test at the 95% significant level (see text for details). This is a relatively stationary seizure. **(b)** Nonstationarity pdf test for UL seizure B typifies a highly nonstationary seizure with few regions of global stationarity.

FIG. 5. **(a)** Average frequency  $\langle\omega\rangle$  versus epoch for BL seizure A. This seizure has a region of uniform average frequency between 12 and 21 seconds. **(b)** Average frequency for unilateral (UL) seizure A. Leads O2 and FP1 never slow down in frequency unlike the other leads.



FIG. 6. **(a)** Mutual information coefficients for BL seizure A demonstrates that (particularly initially) leads T6, O2, FP2, O1, P3, T5, T3, F8, and T4 have relatively lower redundancy compared with the other leads. This suggests that they are late to enter the seizure. At 8 epochs, all leads have improved mutual information. Lower redundancy is seen in occipital and frontal-polar leads throughout the seizure. **(b)** Mutual information coefficients for BL seizure B reveals a low redundancy with CZ even during the 5-epoch global stationary region at the beginning of this seizure.

FIG. 7. **(a)** The linear correlation coefficients between CZ and the other leads of BL seizure A clearly shows that the frontal polar leads FP1 and FP2 are poorly correlated. This is due to large time-delays with CZ. **(b)** The linear correlation coefficients between CZ and the other leads of UL seizure A demonstrates that channels O2 and FP1 are poorly correlated, a result of their higher frequency content. Channels O1 and FP2 have poorer correlations since these leads have large time-delays with CZ.

FIG. 8. **(a)** Average mutual information transmission coefficients calculated for UL seizure C over a multi-lead stationary region located by pdf stationarity tests of 8 seconds. Redundancy is strongest with leads that are in the same hemisphere of the brain. **(b)** Average mutual information coefficients for BL seizure A over a multi-lead stationary segment of 16 seconds by the pdf stationarity test. There is strong redundancy in the frontal portion of the brain. Poor redundancy is seen in the occipital and temporal leads.

FIG. 9. **(a)** Average correlation coefficients of UL seizure A over a multi-lead stationary segment of 16 seconds by the pdf stationarity tests. Channels O2 and FP1 have good correlations with each other but not with other leads on the head due to their having high average frequencies. Channels FP2 and O1 have the same common frequencies with other leads on the head, but have lower correlations due to significant time-delays with spatially distant leads. **(b)** Average correlation coefficients of BL seizure A over a 16 second stationary segment by the pdf stationarity test and uniform frequency. The frontal polar leads have high correlations with the surrounding frontal leads but poor correlation with the occipital and temporal leads. This pattern of time-delay is due to an anterior to posterior time delay (see Fig. 10).

FIG. 10. Time-averaged time-delay for BL seizure A, in the uniform region (Fig. 6a ) from 25 to 45 seconds . The degree of average time-delay is referenced according to the color-bar below the figure. This map, looking down on the top of the head, portrays 19 data points (represented by the "+" symbols) with linear interpolation carried out in between the leads. Note the significant anterior-to-posterior time-delay topography.

Figure 1a:

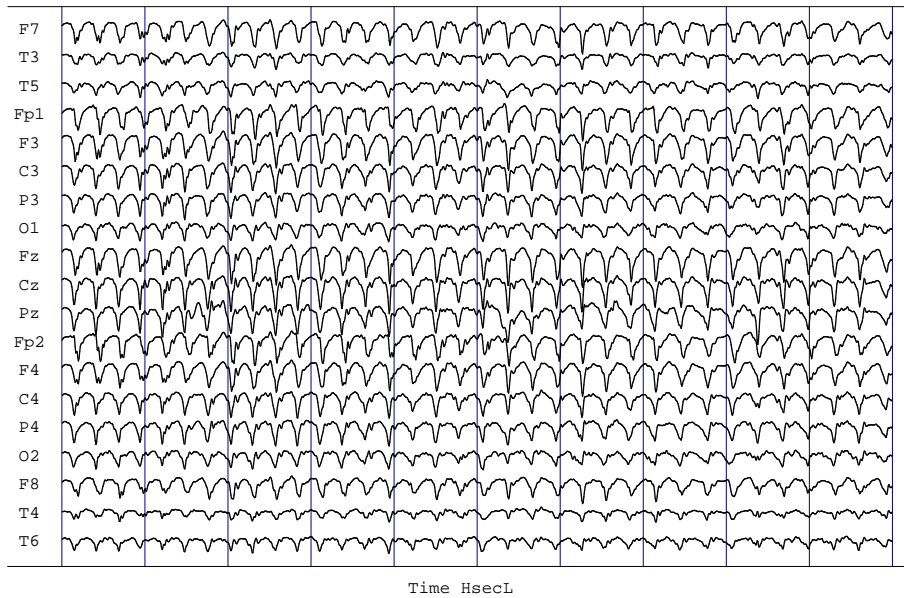


Figure 1b:

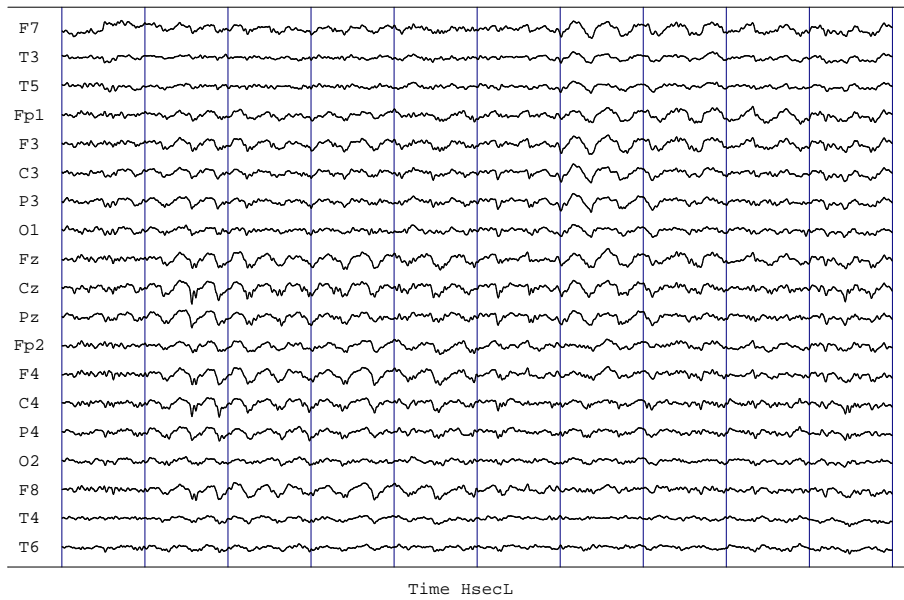


Figure 2:

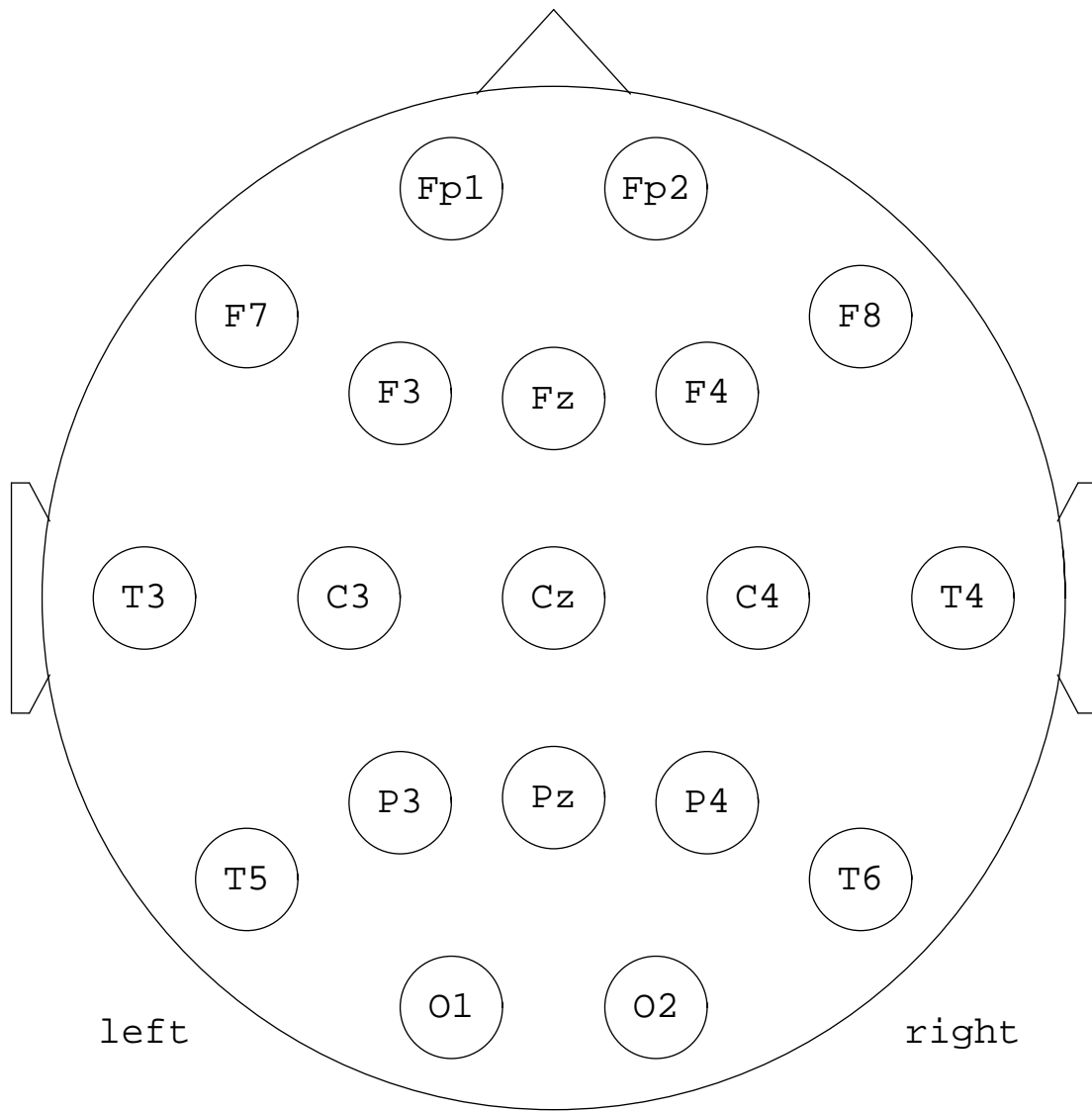


Figure 3a:

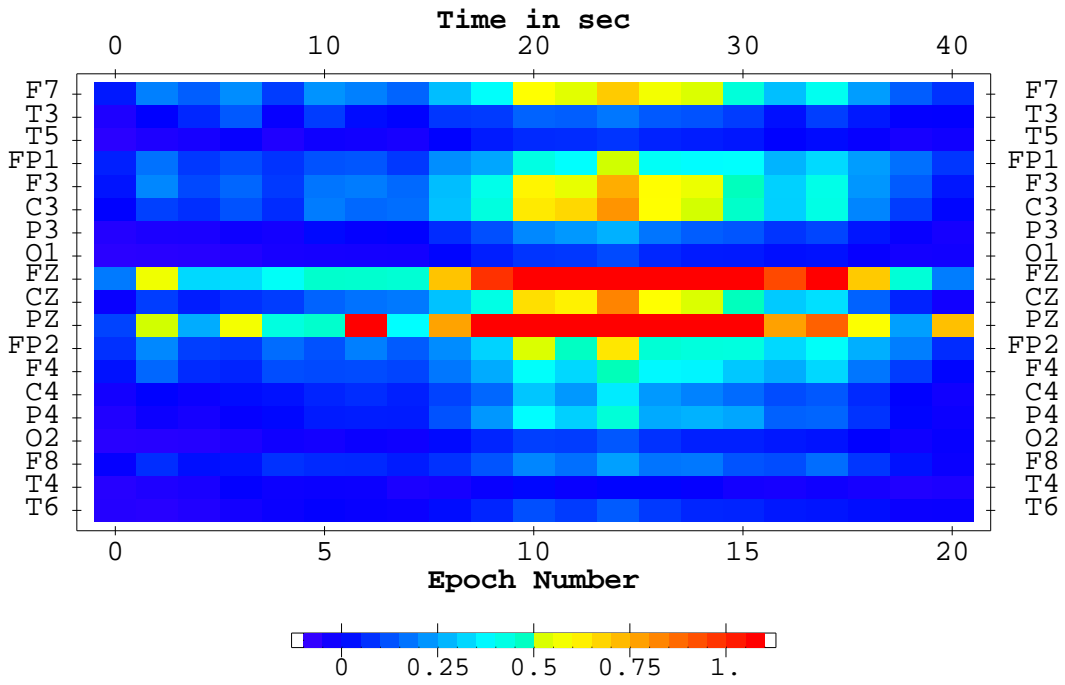


Figure 3b:

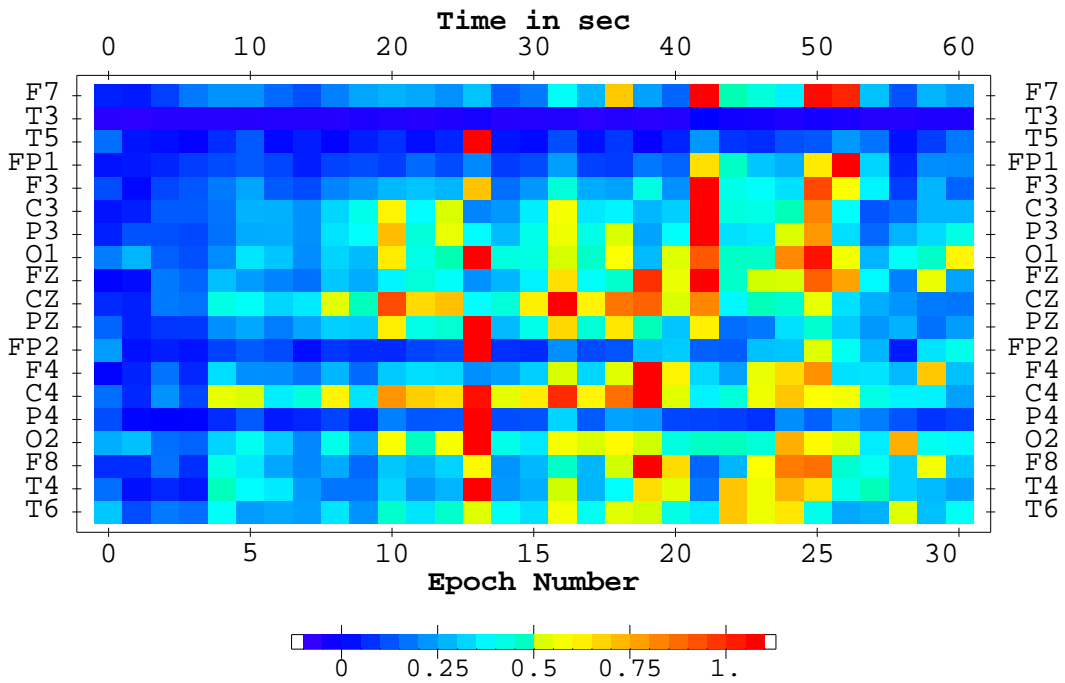


Figure 4a:

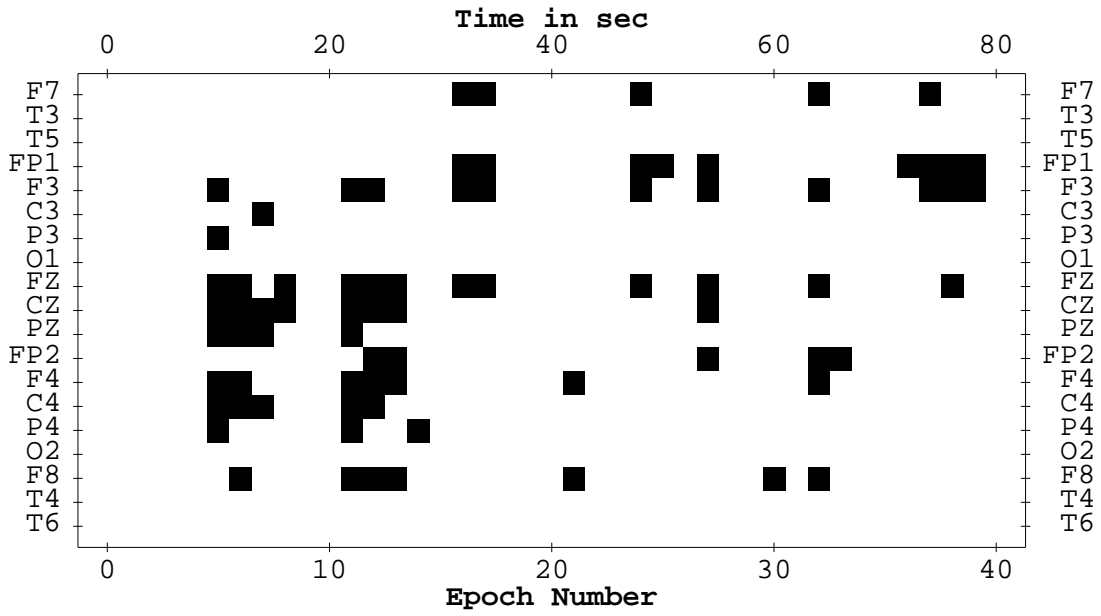


Figure 4b:

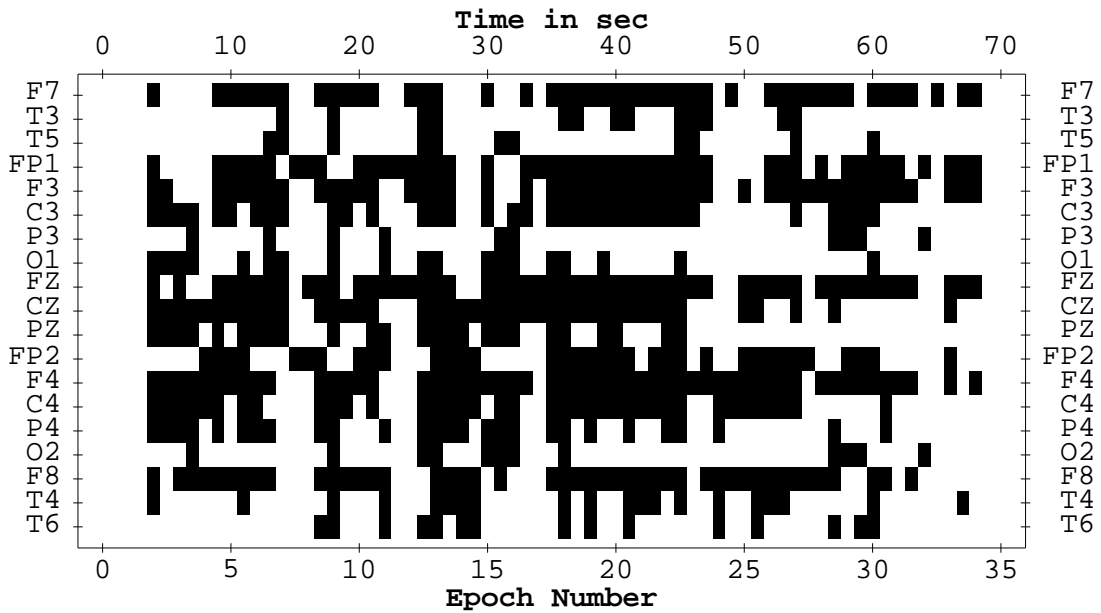


Figure 5a:

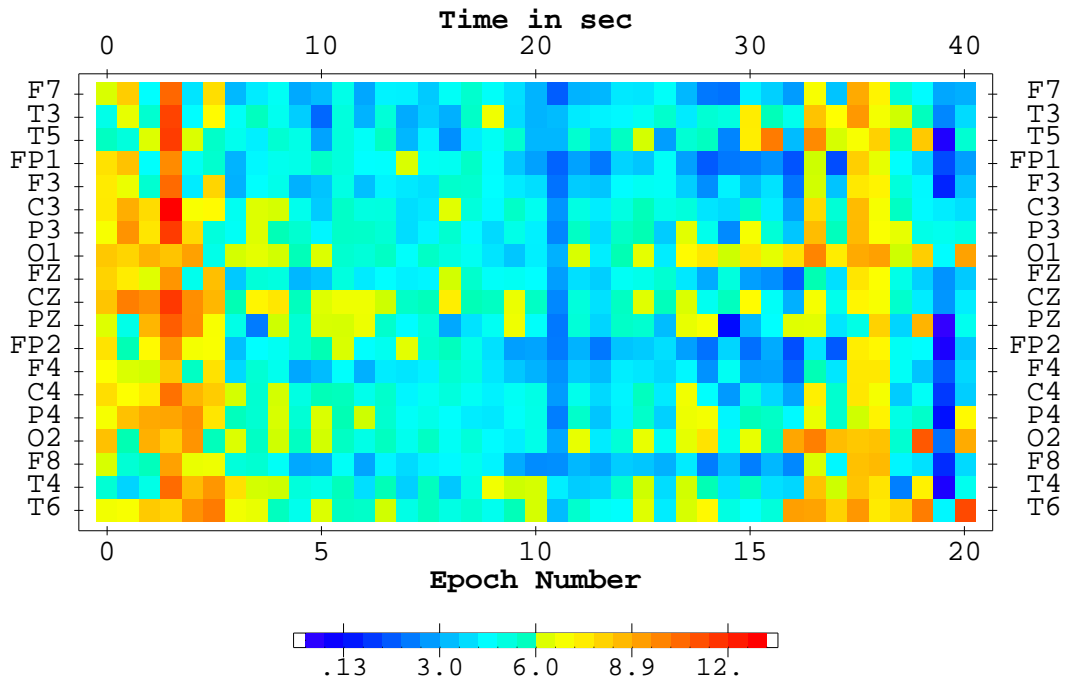


Figure 5b:

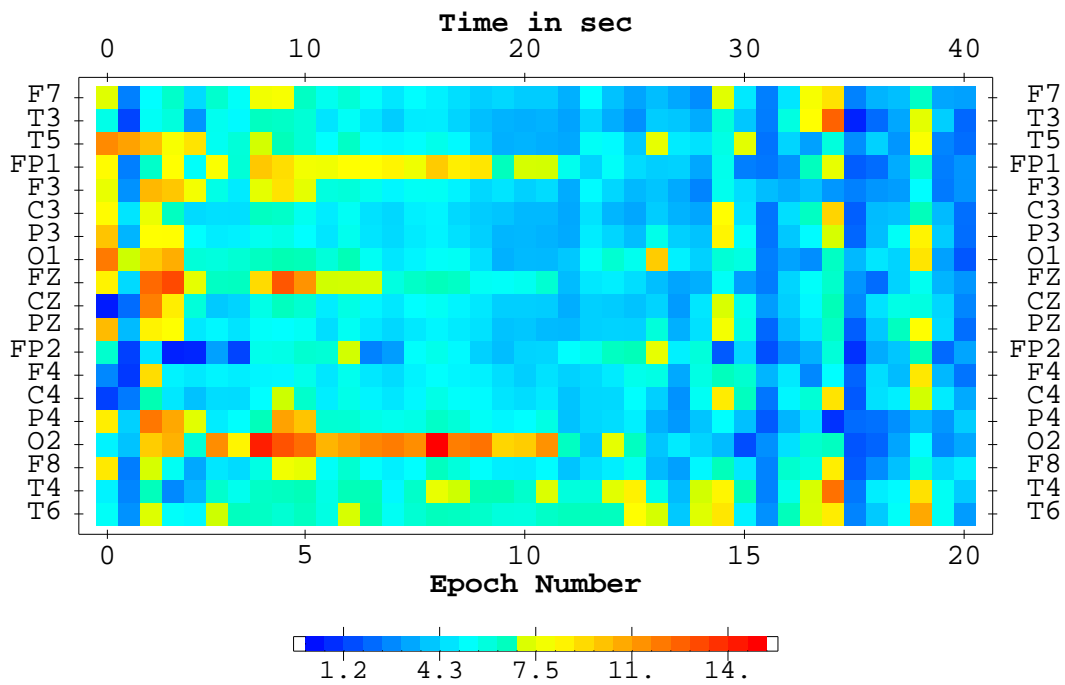


Figure 6a:

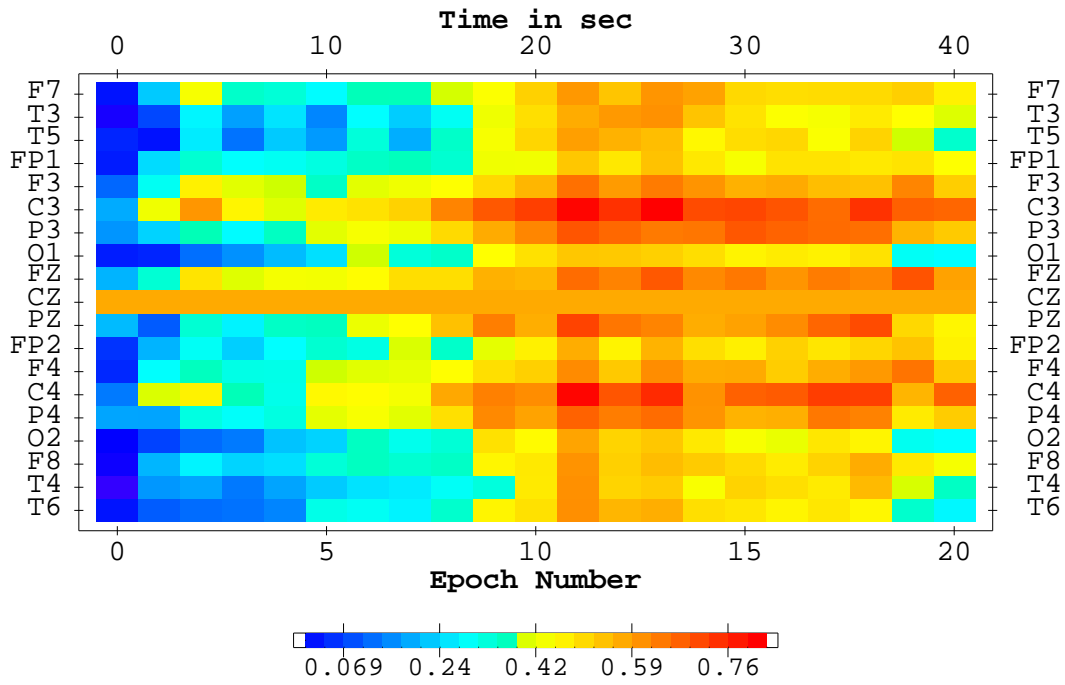


Figure 6b:

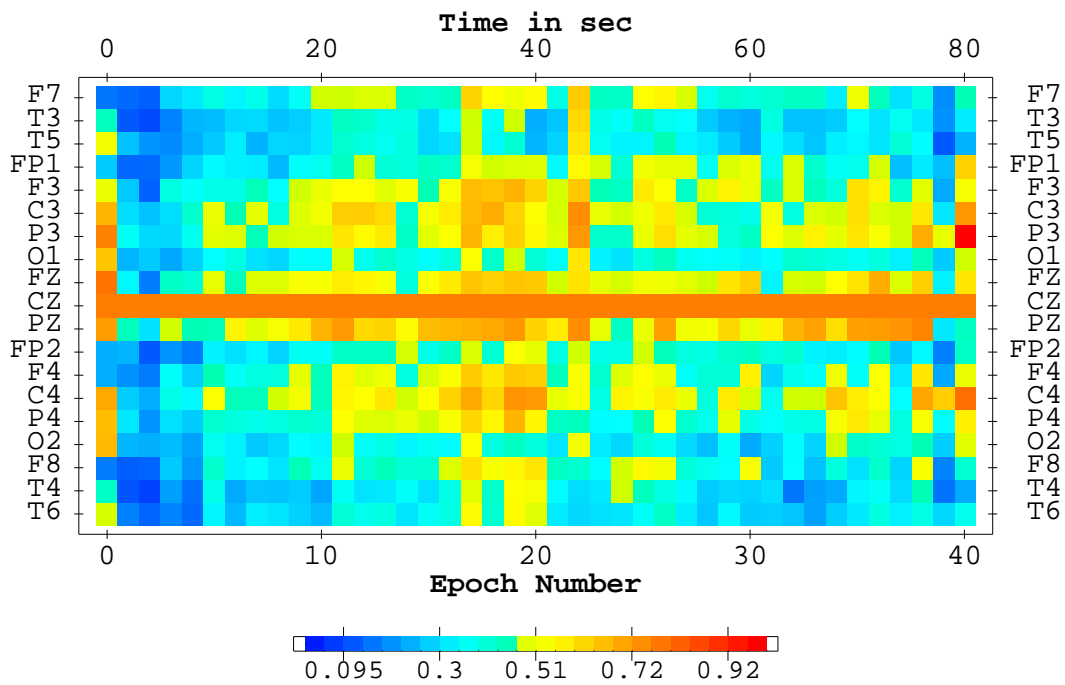




Figure 7a:

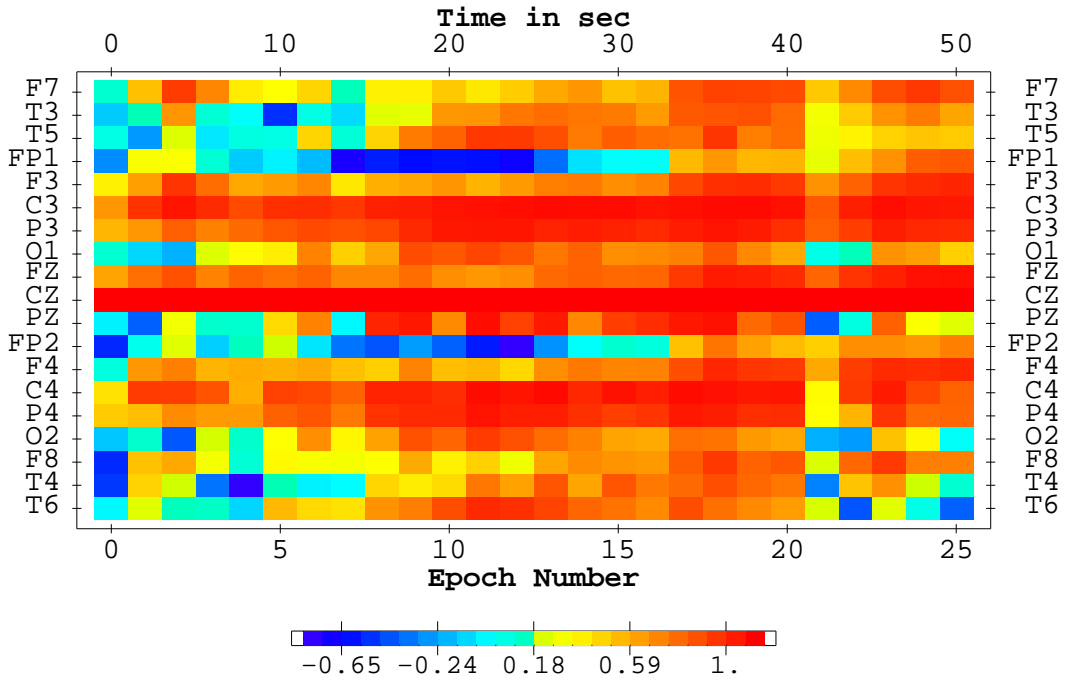


Figure 7b:

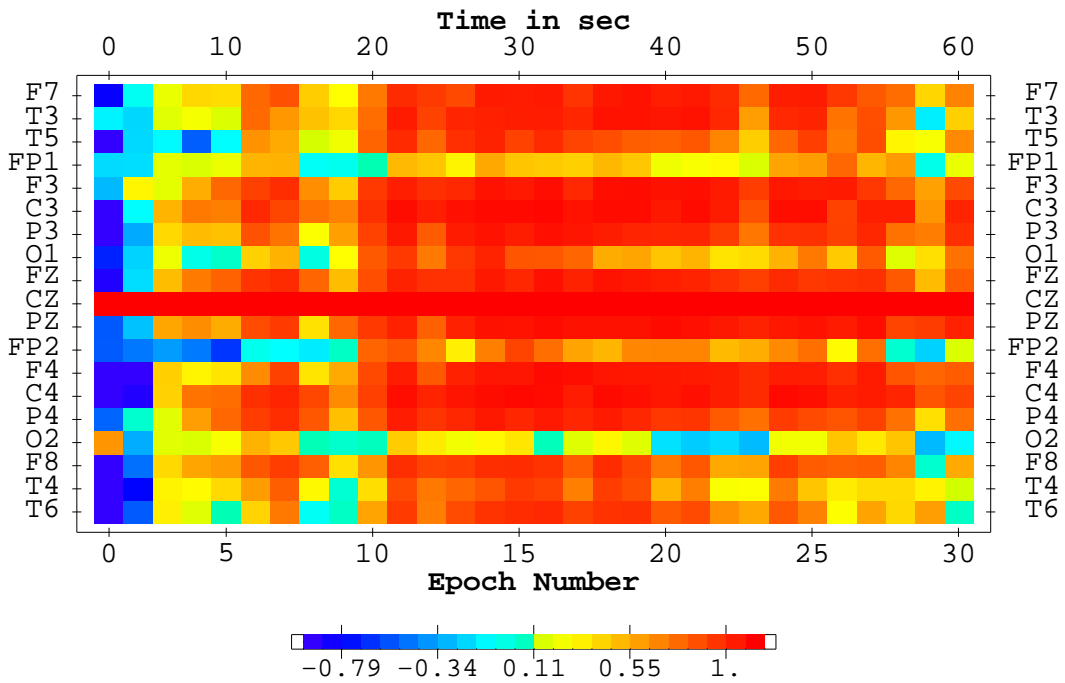


Figure 8a:

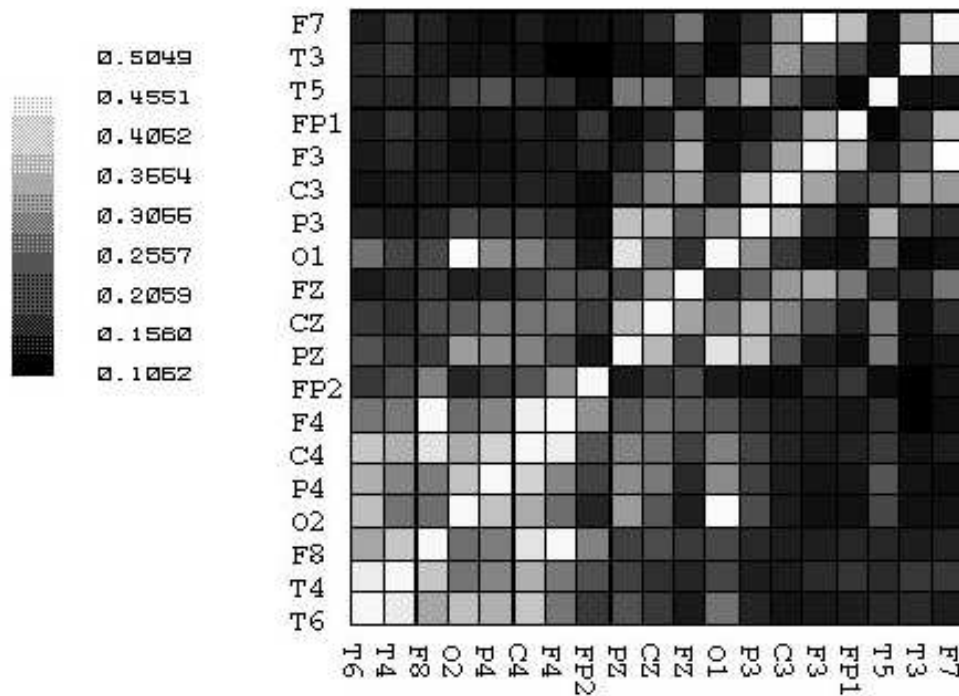


Figure 8b:

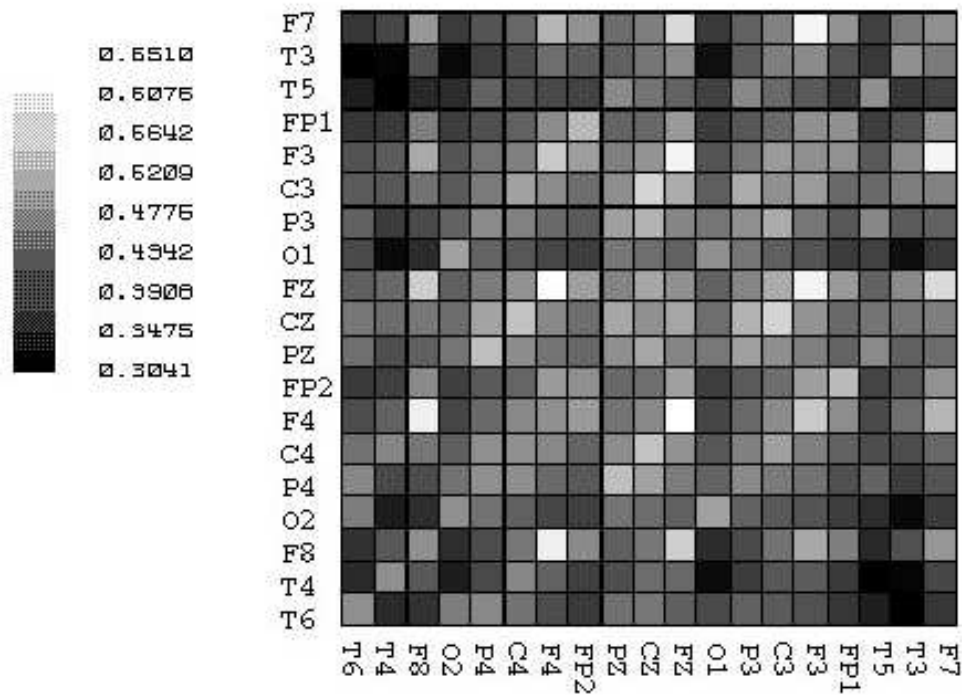


Figure 9a:

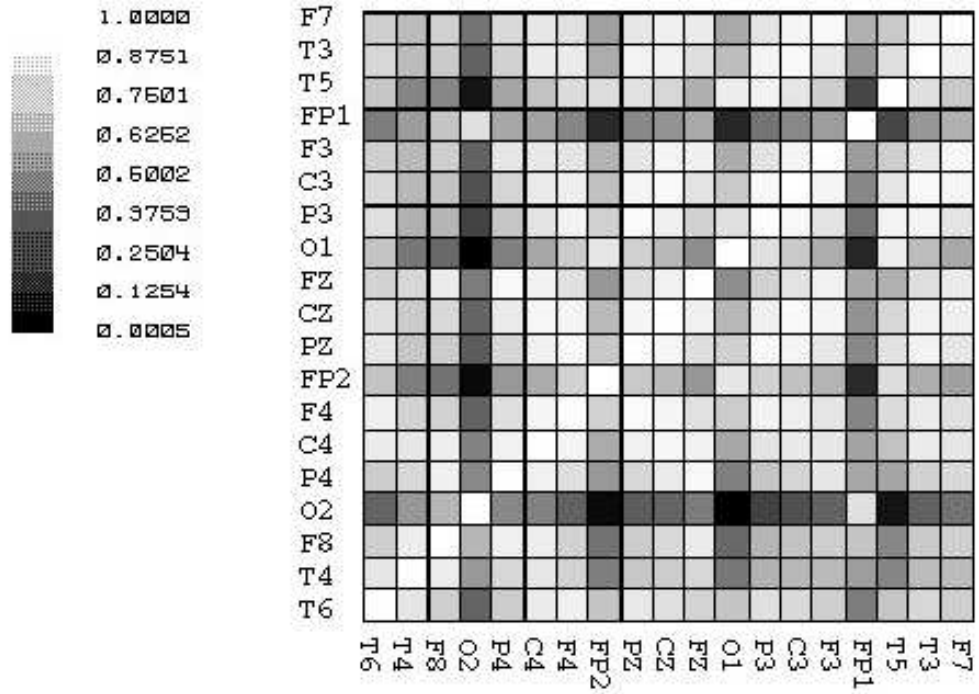


Figure 9b:

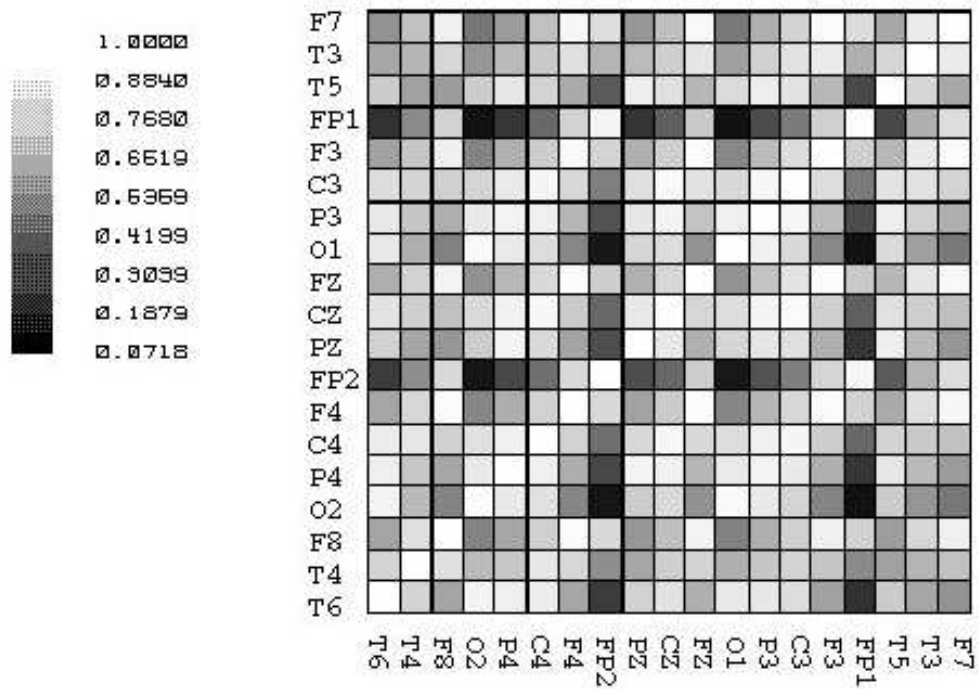


Figure 10:

